Desalination and Water Treatment
www.deswater.com

doi: 10.5004/dwt.2022.28784

271 (2022) 166–175
September

Defluoridation of geothermal water by adsorption onto activated sludge: kinetics, isotherms and thermodynamics studies

Qiangying Zhang[a], Jian Xiong[a], Xiaomei Cui[a], Haishuai Yang[a], Zeng Dan[a], Xuebin Lu[a,b,*], Duo Bu[a,*]

[a]*College of Science, Tibet University, Lhasa 850000, China, Tel. 0891-6405210; email: phudor@vip.163.com*
[b]*School of Environmental Science and Engineering, Tianjin University, Tianjin 300350, China*

Received 27 March 2022; Accepted 24 July 2022

ABSTRACT

In this work, inexpensive, easily available and typical waste activated sludge (generated by anaerobic/anoxic/oxic (A^2/O) and cyclic activated sludge system (CASS) processes) was investigated as an adsorbent for the defluoridation of geothermal water using both batch and column adsorption systems. Initially, the defluoridation efficiency was optimized in batch experiments according to sludge type, contact time, initial F^- concentration and adsorbent dose. Fluoride removal efficiency of A^2/O was superior to that of CASS. An optimum 86% fluoride removal efficiency occurred at an adsorbent dose of 60 g/L within 180 min. The adsorption behaviors were fitted well by the pseudo-first-order model and Freundlich model. Moreover, the thermodynamic parameters illustrated that the adsorption process of fluoride on activated sludge was spontaneous and endothermic. The mechanism of fluoride adsorption was exchange with hydroxyls on the activated sludge. The release of OH^- due to fluoride adsorption was confirmed by the observed pH values. Finally, a homemade column was used to systematically evaluate the defluoridation performance for real F-containing geothermal water. The dynamic adsorption capacity was 0.55 mg/g. The results demonstrated that this simple, economic and efficient sludge adsorbent has potential for application and can be developed into a feasible defluoridation technology for F^- removal from geothermal water.

Keywords: Activated sludge; Adsorption; Defluoridation; Geothermal water

1. Introduction

Geothermal fluids and springs are found around the world. As an important part of the Himalayan geothermal belt, the Tibetan Plateau is the region of China where high temperature hydrothermal systems are intensively distributed. Large numbers of fluoride-enriched geothermal springs are widely distributed on the southern Tibetan Plateau [1]. However, the high temperature hydrothermal systems discharge high fluoride (F^-) to the near river, which implied that fluoride from geothermal water poses a potential threat to the shallow groundwater or surface water [2].

Fluoride is one of the indispensable trace elements for humans and animals, and a lack of F^- can lead to is prone to dental caries. F^- plays a pivotal role in the formation of animal bones and teeth. An appropriate amount of F^- is beneficial for bone and tooth development and dental health. However, excessive intake of F-contaminated water will result in severe diseases such as osteoporosis, dental fluorosis, skeletal fluorosis, and stiffened and brittle bones [3]. In view of the dual effects of F^-, the World Health Organization (WHO) has placed strict requirements on the F^- concentration in drinking water. The WHO recommends a permissible limit of 1.5 mg/L, while China

* Corresponding authors.

has set a stringent guidance value of 1.0 mg/L for F^- [4]. In Tibet, the Yangbajing geothermal spring is a typical high temperature geothermal water, with an F^- concentration as high as 17.4 mg/L [5], which severely exceeds the standard for F^- in surface water. A geothermal power plant is the main source of F^- in adjacent river, and the residual F^- concentration is closely related to wastewater discharge from surrounding geothermal power plants. Therefore, the water pollution in the environmental caused by nearby geothermal activities cannot be ignored. To reduce and prevent the adverse effects of high-fluoride geothermal water, the development of geothermal defluoridation technology is urgently needed. The development of defluoridation technology is of great significance for ensuring the safety of water systems [6].

Great efforts have been made to improve defluoridation technologies, and a variety of available strategies, such as adsorption, precipitation, ion exchange, electrocoagulation, and membrane filtration, have been reported to remove F^- in aqueous solutions [4,7,8] Among these technologies, electrocoagulation is an effective process to remove fluoride from water systems. However, electricity is required to operate the plant which increases its operating cost. It is widely recognized that adsorption is an ideal and appropriate technique compared to other defluoridation technologies, and is characterized by high efficiency, low cost and easy operation [9–11]. The key factor for adsorption is the development of high-performance adsorbents. A series of adsorbents have been employed for F^- removal, such as metal oxides [12–14], zeolite materials [15], and natural materials [16,17]. Low-cost wastes are alternative effective adsorbents to remove F^- from geothermal water for water purification.

It is critical to find a waste adsorbent with low cost and high adsorption capacity to efficiently eliminate fluoride from geothermal water. Because fluoride-enriched geothermal springs are characterized by high temperature, high mineralization, and alkaline pH, the efficient elimination of fluoride is still a major challenge. Activated sludge is a by-product produced by sewage treatment plants, and its safe treatment and disposal are an urgent problems to be solved. Activated sludge is a flocculant contains abundant organic matter and microorganisms, which can provide adsorption sites for F^-, and this material is widely available and low in cost. Therefore, the development of sludge adsorbents plays a positive role in realizing sludge recycling and promoting the development of sludge treatment and sustainable disposal technology. Activated sludge has been used to developed effective adsorbents for dyes [18], estrogens [19], and heavy metals [20,21]. Activated sludge is suggested herein as an ideal candidate material for use as a low-cost adsorbent for the removal of F^- from geothermal water systems.

The overall objective of this research was to evaluate the defluoridation potential of activated sludge, a waste by-product of sewage treatment plants. Fluoride adsorption experiments were performed considering contact time, initial F^- concentration, and adsorbent dose. Attempts were also made to understand the adsorption kinetic, adsorption isotherm, adsorption thermodynamic and mechanism. The experimental results showed that the activated sludge has application potential for the removal of fluoride from geothermal water.

2. Materials and methods

2.1. Instruments and reagents

The concentration of F^- was determined by an ION 700 fluoride meter (Youte Instrument Co., Ltd., China). A pHSJ model pH meter (Shanghai Yidian Scientific Instrument Co., Ltd., China). ZNCL-G190*90 constant temperature water bath magnetic stirrer (Hefei Yuhua Instrument Co., Ltd., China), and BSA224S electronic analytical balance (Sartorius, Germany) were used for the adsorption experiments. Activated sludge from anaerobic/anoxic/oxic (A^2/O) and cyclic activated sludge system (CASS) processes was obtained from a wastewater treatment plant (Lhasa, Tibet). Total ionic strength buffer (TISAB) and 100 mg/L NaF standard solution (Thermo Scientific Orion, USA) were employed for F^- determination.

2.2. Characterization of the adsorbents

The activated sludge was characterized by Fourier-transform infrared spectroscopy (FT-IR), powder X-ray diffraction (XRD), scanning electron microscopy (SEM), and Brunauer–Emmett–Teller (BET) surface area analysis. The XRD patterns of the activated sludge were obtained on a D8 ADVANCE X-ray diffractometer (Bruker, Germany) with Cu Kα radiation (k = 1.5406 Å). The surface morphology of activated sludge were obtained using SEM (FEI-SEM, Japan). The surface areas and pore size distribution were measured by N_2 adsorption–desorption isotherms (ASAP 2020, Micromeritics, USA), after all the activated sludge was degassed. The infrared spectra were recorded on a Nicolet 6700 FT-IR spectrophotometer (Thermo Scientific, USA), the dry activated sludge was mixed with KBr powder, and then measured from 4,000 to 400 cm^{-1} with a resolution of 4 cm^{-1}.

2.3. Batch and column experiments

Parallel experiments were carried out to investigate the adsorption performance of the sludge for F^-. Specifically, 1.2 g of the dry sludge was added to 30 mL geothermal water and stirred at 80°C for 180 min to reach equilibrium. The defluoridation efficiency was optimized according to the sludge type, adsorbent dose (5, 10, 20, 30, 40, 50, and 60 g/L), contact time (5, 10, 20, 30 and 240 min) and initial F^- concentration (1, 2, 5, 10 and 20 mg/L) in batch experiments. In the column experiment, 1.5 g of the sludge was added and washed until F^- in the effluent could not be detected. After sampling, the concentration of F^- in the effluent was determined.

The determination of fluoride was based on the ion selective electrode method. Accordingly, the electrode potential E (mV) and the concentration of F^- in solution correspond to the Nernst equation. The stock F^- standard solution of 100 mg/L was stepwise diluted to 0.5, 1, 5, 10 and 50 mg/L. Then, 3 mL TISAB was added to 3 mL F^- standard solutions. After mixing, E (mV) was measured. The linear regression between E and $-\lg C_{F^-}$ was fitted, and the regression equation ($E = k(-\lg C_{F^-}) + b$, $y = 59.37x + 92.91$) and correlation coefficient

(R^2 = 0.9972) were obtained. The F^- concentrations were calculated from the calibration curve.

2.4. Geothermal water collection

Yangbajing geothermal water was collected on June 20, 2019. The geographical location of the sampling point is shown in Fig. 1. Conventional water quality parameters, including water temperature, pH, conductivity, total dissolved solids, and salinity, were measured in the field. Furthermore, the concentrations of common cations (Ca^{2+}, Mg^{2+}, K^+, and Na^+) and anions (Cl^-, SO_4^{2-}, CO_3^{2-}, HCO_3^- and F^-) in the geothermal water are presented in Table 1.

3. Results and discussion

3.1. Characterization

The SEM images in Fig. 2a–f show the micromorphology of the sludge before adsorption of F^-. The sludge presented a dense blocky surface structure and irregular small particles adsorbed on the surface. The surface structure was dense without pores. The average particle size for the two sludge was 4 μm. Fig. 2g shows the FT-IR spectrum of the sludge before adsorption of F^-. Differences were not readily apparent in the positions of the absorption bands, but their relative intensity exhibited clear differences. The broad peak near 3,300 cm^{-1} was related to the N–H stretching vibrations of protein [22], and the absorption peaks at 2,921 and 2,850 cm^{-1} were caused by the asymmetric and symmetric stretching vibrations of CH_2 in lipids. The absorption peak at 1,658 cm^{-1} correspond to the stretching vibration of COO^- in peptides and proteins. The peaks at 1,542 and 1,452 cm^{-1} represent NH_3^+ and C–H bonds in peptides and polysaccharides. The absorption peak at 1,034 cm^{-1} was produced by the stretching vibration of the C–O bond in glycerin [23]. FT-IR analysis showed that the absorption peaks of COO^- and other characteristic functional groups may be related to the extracellular polymeric substances (EPS) in the activated sludge. As important constituents of activated sludge flocs, EPS plays significant roles in pollutant adsorption [22]. Most likely, EPS contains a large number of hydroxyl, carboxyl and aldehyde groups, which are the main functional groups that combine with F^-.

The XRD patterns in Fig. 2h were consistent with those obtained in recent studies [24]. Apparently, the diffraction peaks at 2θ values from 20° to 30° were consistent with clay [25]. As shown in Fig. 2i, the nitrogen adsorption/desorption isotherm curve showed a low specific surface area (S_{BET}) and pore volume. The S_{BET} values for A^2/O and CASS sludge were estimated to be 1.51 and 1.18 m^2/g, respectively. The Barrett–Joyner–Halenda (BJH) adsorption average pore diameters of A^2/O and CASS sludge were 16.11 and 16.44 nm, respectively. The samples had mainly dense structures and were mostly nanoporous, so the specific surface area was relatively low, which coincided with the SEM data.

3.2. Effect of sludge type

The F^- removal efficiency of the activated sludge from the A^2/O and CASS processes was compared. As shown in Fig. 3, the removal efficiency of activated sludge from the A^2/O process was approximately 1.8 times higher than that of the CASS process under the same conditions. Generally, activated carbon is added as a microbial carbon source in the A^2/O sewage treatment process, so residual activated carbon was inevitably remains in the sludge. Additionally, the A^2/O activated sludge exhibited a relatively high specific surface area. It is well known that a high specific surface area of adsorbents usually leads to high fluoride removal efficiency, and residual activated carbon doping can increase the specific surface area. A^2/O activated sludge integrates the advantages of a high surface area, which can synergistically contribute to a high fluoride removal efficiency. The results showed that the fluoride can

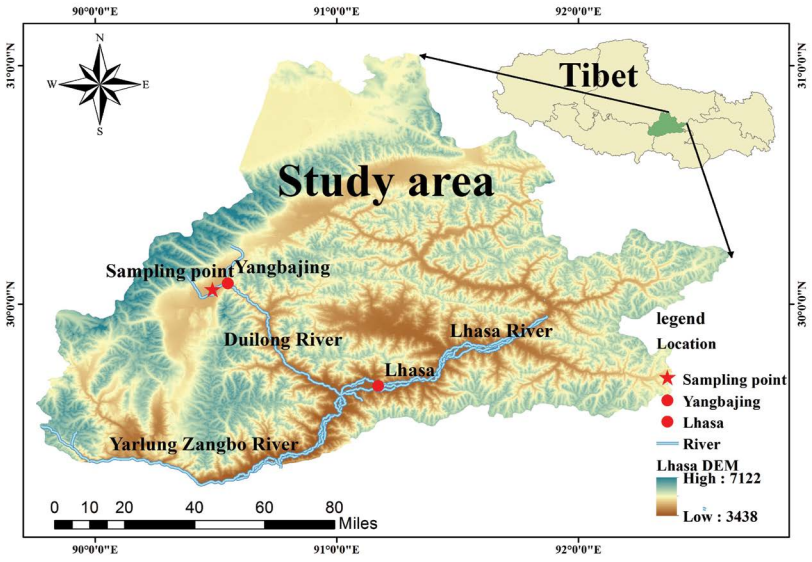

Fig. 1. Geographical location of the sampling point.

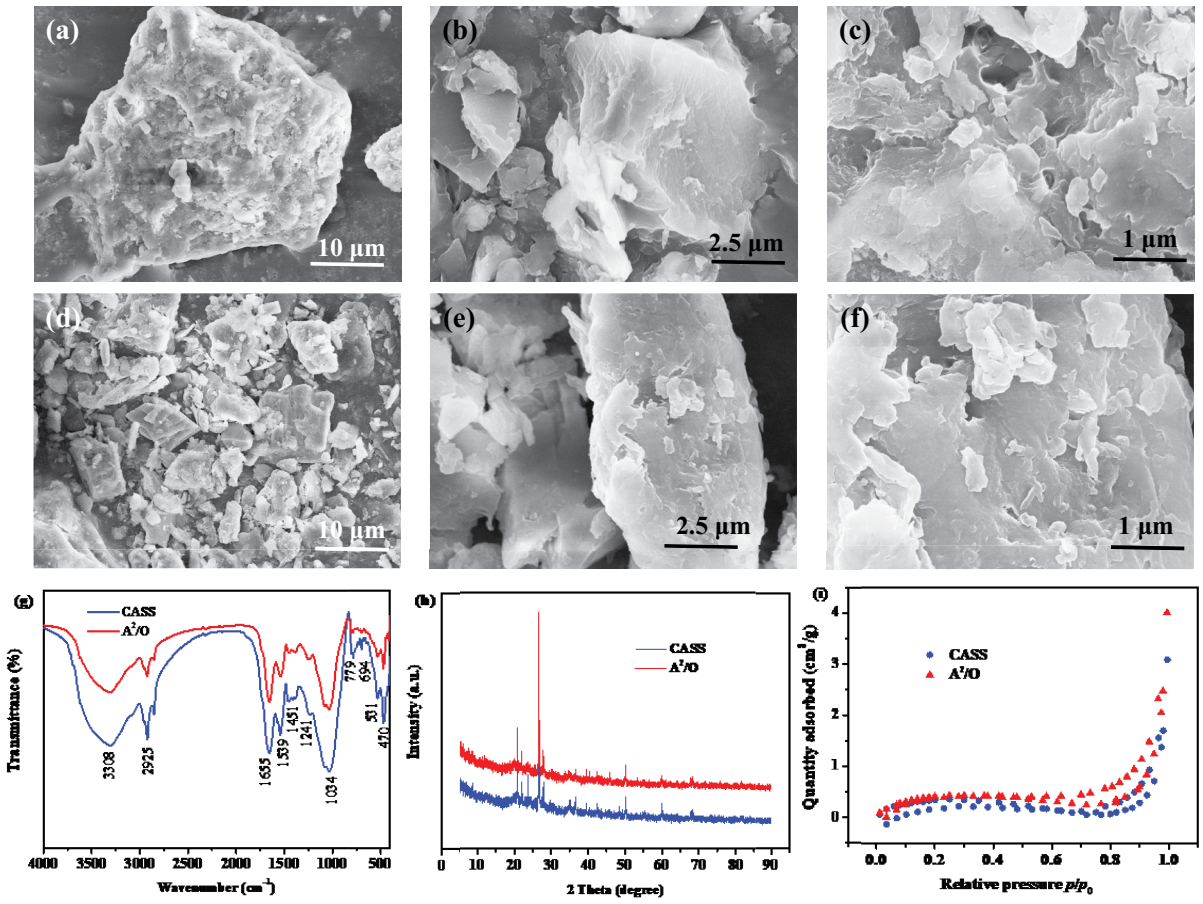

Fig. 2. SEM images of A²/O (a–c) and CASS (d–f), FT-IR spectra (g), XRD patterns (h) and nitrogen adsorption/desorption isotherms (i) of sludge before adsorption of F^-.

Table 1
Conventional water quality parameters of geothermal water collected in Yangbajing geothermal power plant in Tibet, China

Sample	Temperature (°C)	pH	Conductivity (μS/cm)	Total dissolved solids (mg/L)	Salinity (mg/L)	Na^+ (mg/L)	Ca^{2+} (mg/L)
Geothermal water	63	8.95	1,670	1,213	935	328.5	31.45
	Mg^{2+} (mg/L)	K^+ (mg/L)	F^- (mg/L)	Cl^- (mg/L)	SO_4^{2-} (mg/L)	CO_3^{2-} (mg/L)	HCO_3^- (mg/L)
	5.66	47.02	14.65	313.2	229	0	262.3

be adsorbed by the two sludge samples, but has a better affinity for A²/O activated sludge.

3.3. Effect of adsorbent dose

Adsorbent dose is one of the important parameters affecting removal performance, which is mainly related to in the number of adsorption sites. As the adsorption dose increases, the number of adsorption sites increases, and the removal rate of fluoride increases accordingly. In contrast, as the adsorption dose decreases, the number of adsorption sites decreases, and the number of remaining fluoride increases. It is worth mentioning that activated sludge is mostly nanoporous and heavy, so it is often necessary to increase the adsorption dose to achieve a high fluoride removal efficiency. Therefore, the effect of adsorbent dose on F^- removal efficiency was optimized. As illustrated in Fig. 4a, fluoride adsorption depended greatly on the adsorbent dose. An optimum 86% fluoride removal efficiency occurred at an adsorbent dose of 60 g/L. Significantly, the residual F^- concentration dramatically decreased from 14.45 to 2.32 mg/L as the dose increased from 5 to 60 g/L. From a practical perspective, when the adsorbent dose exceeded 50 g/L, the mixed sludge solution was difficult to separate. Fortunately, the fluoride removal percentage was maintained at 68% at an adsorbent dose of

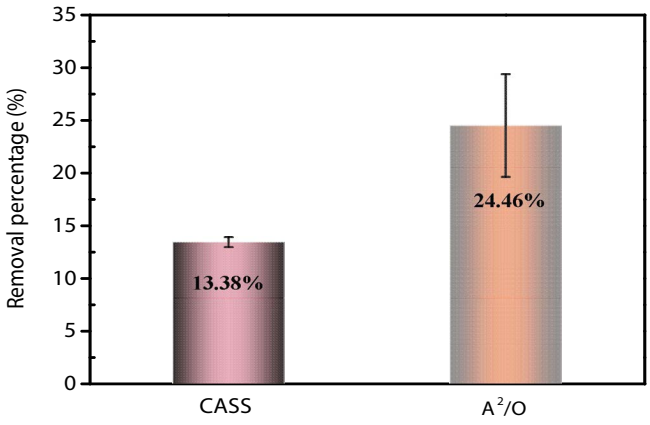

Fig. 3. F^- removal efficiency of the activated sludge.

40 g/L. Thus, 40 g/L was selected as the optimal adsorbent dose.

3.4. Effect of contact time

Contact time is another important parameter determining removal performance. If the contact time is too short, the reactants will not be fully contacted, resulting in incomplete adsorption. When the contact time is too long, the adsorption efficiency will not be greatly improved, and the adsorption process will be time-consuming. Fig. 4b displays the time-dependent F^- removal efficiency of the activated sludge. Specifically, the adsorbent initially exhibited rapid uptake of F^-, followed by slow uptake, and then finally gradually reached equilibrium. Approximately 50% of fluoride adsorption was achieved within the first 60 min, and the time required to reach equilibrium was approximately 180 min. Compared with the equilibrium time of other reported defluoridation adsorbents (as long as 24 h) [26], the adsorption equilibrium time for this sludge was fast. To clearly represent the effect of contact time effect on the F^- removal efficiency of the activated sludge, the residual F^- concentrations are shown. Regardless of the removal efficiency and residual F^- concentration, there were no significant changes after 180 min.

3.5. Effect of initial concentration

The static adsorption capacity is the saturated adsorption capacity of the target ion (F^-) on the adsorbent (sludge), and it is an important parameter to evaluate the performance of adsorbents. The removal efficiency and adsorption capacity of F^- at initial concentrations of 1, 2, 5, 10 and 20 mg/L were investigated and are shown in Fig. 4c. A high adsorption capacity was achieved as increasing initial concentration. Notably, the fluoride level was reduced from the initial concentration of 5.0 to 1.5 mg/L by adding 1.2 mg of sludge. The permissible limit for fluoride in drinking water is fixed at 1.5 mg/L by the WHO. As the F^- concentration increased from 10 to 20 mg/L, the removal efficiency decreased from 74.2% to 57.6% due to the limited number of active sites.

3.6. Adsorption kinetics

The F^- adsorption kinetics by activated sludge were simulated by the linearized form of the pseudo-first-order [Eq. (1)] and pseudo-second-order [Eq. (2)] models [12,27] to identify the rate and kinetics.

$$\text{Pseudo-first-order model: } \log\left(q_e - q_t\right) - \log q_e - \frac{k_1}{2.303}t \quad (1)$$

$$\text{Pseudo-second-order model: } \frac{t}{q_t} = \frac{1}{k_2 q_e^2} + \frac{t}{q_e} \quad (2)$$

where k_1 (min^{-1}) and k_2 (g mg^{-1} min^{-1}) are the rate constants for the two kinetics models and q_e and q_t are the F^- adsorption capacity (mg/g) at equilibrium and at time t (min), respectively.

The obtained adsorption data were fitted to the pseudo-first-order and pseudo-second-order kinetic models, respectively. As concluded in Fig. 5, the experimental results are better fitted by the pseudo-first-order model than the pseudo-second-order model. To present the fitted results more intuitively, the relevant kinetic parameters and correlation coefficients (R^2) are listed in Table 2. The R^2 for the pseudo-first-order kinetic model is quite high (>0.99), and the calculated q_e is reasonable. The adsorption capacity calculated by the pseudo-first-order model (0.24 mg/g) is in extremely good agreement with the experimental value (0.25 mg/g). Obviously, the F^- adsorption data are modeled more consistently with the pseudo-first-order model, indicating the occurrence of physical combination between F^- and adsorption sites on the activated sludge.

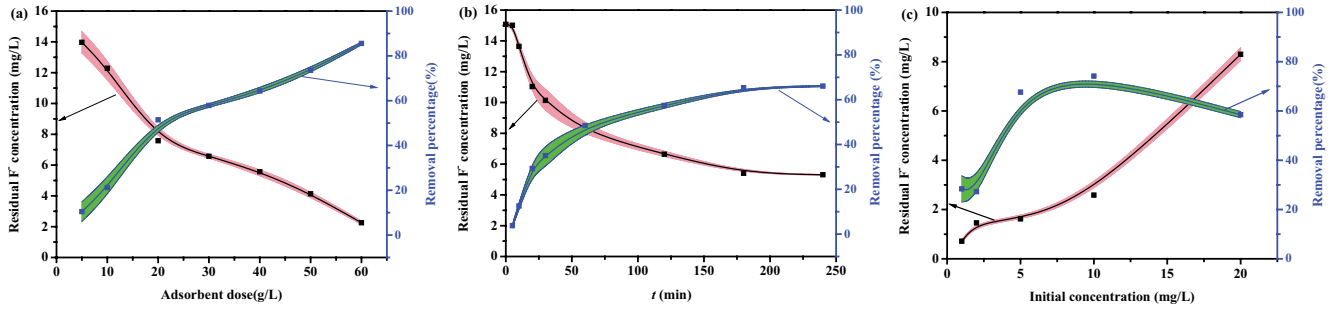

Fig. 4. Effect of adsorbent dose (a), contact time (b) and initial concentration (c) on fluoride removal.

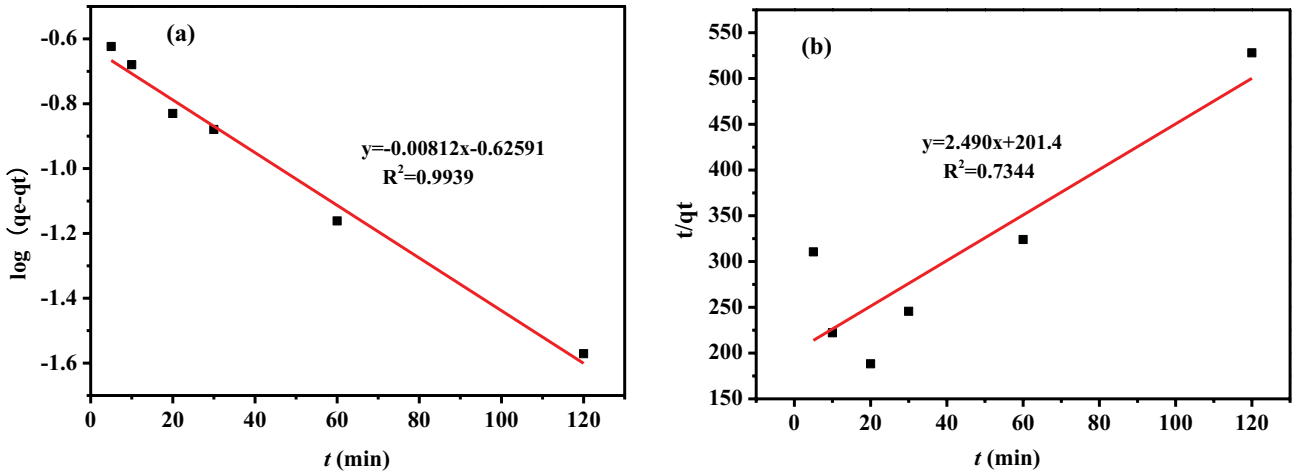

Fig. 5. Adsorption kinetics of pseudo-first-order (a) and pseudo-second-order (b) models.

Table 2
Relevant adsorption kinetic parameters

	Pseudo-first-order				Pseudo-second-order		
	$q_{e,exp}$ (mg/g)	$q_{e,cal}$ (max) (mg/g)	k_1 (g mg^{-1} min^{-1})	R^2	$q_{e,cal}$ (max) (mg/g)	k_2 (g mg^{-1} min^{-1})	R^2
F^-	0.25	0.24	0.0187	0.9939	0.40	0.0308	0.7344

3.7. Adsorption isotherm

Analysis of isotherm data is important for predicting the adsorption capacity of activated sludge, which is one of the main parameters required for the design of an adsorption system. To better understand the adsorption mechanism of F^- and quantify the adsorption capacity, the Langmuir and Freundlich adsorption isotherms were applied to describe and calculate the adsorption process [28]. The Langmuir model assumes that the target (F^-) occupies only one type of active site, consequently forming a monolayer on the adsorbent surface, and the adsorption is monolayer and localized. In contrast, the Freundlich isotherm model assumes a heterogeneous sorption process and the mechanism of retention by physical adsorption [29]. The Langmuir and Freundlich isotherms were calculated using the following equations [12,28]:

$$\text{Langmuir: } \frac{C_e}{q_e} = \frac{1}{bq_{\max}} + \frac{C_e}{q_{\max}} \quad (3)$$

$$\text{Freundlich: } \log q_e = \log K_F + \frac{1}{n}\log C_e \quad (4)$$

where q_e (mg/g), $q_{\max}$ (mg/g) and b (L/mg) are the amount of F^- adsorbed at equilibrium, the maximum adsorption capacity and the Langmuir constant, respectively. k (mg/g) and n are constants that represent the adsorption intensity of the Freundlich model, and a higher n ($n > 1$) indicates that the adsorption process is favorable.

The adsorption experimental data were analyzed and the fitting results are listed in Fig. 6. Additionally, the relevant parameters fitted by the adsorption isotherms are summarized in Table 3. Fig. 6 clearly shows that the fitting result for the Langmuir model is very poor. The adsorption process for F^- by activated sludge is more consistent with the Freundlich adsorption model, according to the higher correlation coefficient (0.9672). The Freundlich model assumes that the process of adsorption occurs on a heterogeneous surface by multilayer deposition and that interactions occur between F^- ions at adjacent sites. Unfortunately, it is difficult to obtain the value of $q_{\max}$ from the Freundlich isotherm model, and only the variable n related to the adsorption intensity can be obtained. The value of n is 0.5912, which is indicative of unfavorable adsorption. Overall, F^- adsorbed on the activated sludge surface was fitted by the Freundlich model, confirming the heterogeneity of the sludge surface and indicating multilayer adsorption.

3.8. Adsorption thermodynamics

The fluoride adsorption behavior of the activated sludge was investigated at five different temperatures from 298.15 to 353.15 K. To determine the thermodynamic feasibility and confirm the nature of the adsorption process, three basic thermodynamic parameters, standard free energy ($\Delta G°$), the standard enthalpy ($\Delta H°$) and standard entropy ($\Delta S°$), were calculated using Eqs. (5)–(7) [30,31].

$$K_0 = \frac{C_e}{q_e} \quad (5)$$

Table 3
Relevant adsorption isotherm parameters

	Langmuir				Freundlich		
	$q_{e,exp}$ (mg/g)	$q_{e,cal}$ (max) (mg/g)	b (L/mg)	R^2	k	n	R^2
F^-	0.29	0.24	0.0187	0.0837	0.0197	0.5912	0.9672

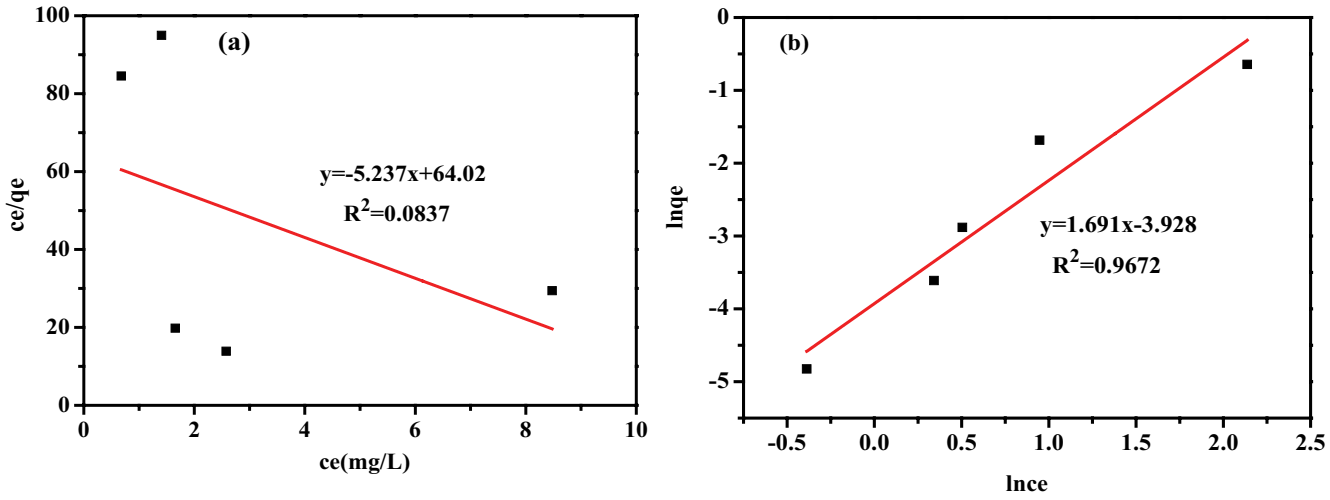

Fig. 6. Adsorption isotherm of Langmuir (a) and Freundlich (b) isotherm models.

$$\Delta G^\circ = -RT\ln K^\circ \quad (6)$$

$$\ln K^\circ = \frac{\Delta S^\circ}{R} - \frac{\Delta H^\circ}{RT} \quad (7)$$

where R is the universal gas constant (8.314 J/mol K) and T is the Kelvin temperature (K). The values of ΔS° and ΔH° were obtained from the intercept and slope of the plot of $\ln K^\circ$ vs. $1/T$ from Eq. (7). The linear regression between $\ln K^\circ$ and $1/T$ is fitted in Fig. 7. The values of the above stated parameters are compiled in Table 4. The negative ΔG° value indicates the spontaneous nature of the adsorption process. The value of ΔH° for fluoride adsorption is 4.989 kJ/mol, suggesting that the interaction between fluoride on activated sludge is endothermic in nature. Further, the positive value of ΔS° (44.575 J/mol) indicates the affinity of the sludge for fluoride.

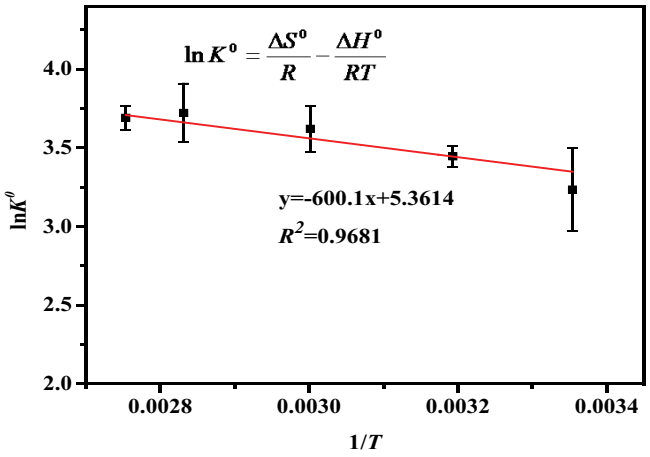

Fig. 7. Thermodynamics plot for fluoride removal onto the activated sludge.

3.9. Removal mechanism

The adsorption isotherm and adsorption kinetics data show that F^- adsorption was mainly based on physical adsorption. The hydroxyl groups of EPS in sludge obviously play important roles in the fluoride adsorption. Given the infrared characterization results, the adsorption mechanism for F^- was mainly electrostatic interactions. At acidic pH values, hydroxyl groups were protonated, and electrostatic interactions occurred. A possible reaction mechanism for the adsorption of fluoride onto the sludge can be hypothesized as follows:

$$\equiv \mathrm{EPS-OH(s)} + \mathrm{H^+} + \mathrm{F^-(aq)} \longleftrightarrow \equiv \mathrm{EPS-OH_2^+ - F^-(s)} + \mathrm{H_2O} \quad (8)$$

However, as the pH of the geothermal water was 8.95, fluoride adsorption was possibly dominated by ion exchange at alkaline pH values. The pH value of the solution after adsorption was measured to determine whether there was OH^- release. As expected, the pH of the solution after adsorption increased to 9.20, which confirmed that OH^- was released due to fluoride adsorption. The mechanism of fluoride adsorption was exchange with hydroxyls on EPS

in the sludge. The ion exchange mechanism can be briefly illustrated as follows:

$$\equiv \mathrm{EPS-OH(s)} + \mathrm{F^-(aq)} \longleftrightarrow \equiv \mathrm{EPS-F(s)} + \mathrm{OH^-(aq)} \quad (9)$$

As presented in Fig. 8, the F^- removal mechanism mainly involves ion exchange and electrostatic interactions.

3.10. Treatment of real F-containing geothermal water

To investigate the application effect of sludge in the actual removal process, a dynamic solid-phase column was investigated [32]. Specifically, the 1.5 g sludge was placed into a 20 mL injection tube. Geothermal water with an initial concentration of 14.65 mg/L (denoted as C_0) was passed through the microcolumn at a flow rate of 0.7 mL/min. The concentration of the effluent was measured and recorded as C_t. The variation curve of C_t/C_0 and dynamic adsorption capacity are shown in Fig. 9. As shown in Fig. 9a, when the sample loading time exceeded 30 min, the ratio of C_t/C_0 was approximately 0.1, and the residual F^- concentration exceeded the recommended value of the WHO (1.5 mg/L). After 170 min, the ratio of C_t/C_0 gradually increased to 0.9, and the dynamic adsorption capacity was calculated to be 0.55 mg/g (Fig. 9b). A comparison of the adsorption capacities with waste-derived activated carbon adsorbents is presented in Table 5. Compared with activated carbon [33,34], red mud [35], and sludge [36], the F^- adsorption capacity of the sludge in this study was higher, while the capacity of the activated sludge adsorbent was slightly lower than those obtained with previously reported waste adsorbents [37–42]. However, activated sludge has abundant sources and the benefits of low cost and no need for a complicated modification process, making it an efficient potential adsorbent for removing F^- from aqueous solution.

Table 4
Thermodynamic parameters for the removal of fluoride

T (K)	$\Delta G°$ (kJ/mol)	$\Delta H°$ (kJ/mol)	$\Delta S°$ (J/mol)
298.15	–8.02		
313.15	–8.97		
333.15	–10.03	4.989	44.575
353.15	–10.93		
353.15	–11.14		

4. Conclusion

Here, sludge from both A^2/O and CASS processes was reported to be potential adsorbent for the removal of F^- from water. Sludge from the A^2/O process had better adsorption performance for F^- than that from the CASS process. The activated sludge was capable of removing 90% F^- within 180 min using an adsorbent dose of 60 g/L. The adsorption of F^- by sludge conforms to the pseudo-first-order model and Freundlich isotherm model. The mechanism of fluoride adsorption was exchange with hydroxyls on EPS compounds in the sludge. Notably, the fluoride level was reduced from the initial concentration of 5.0 to 1.5 mg/L by adding 1.2 g of sludge. Activated sludge from the A^2/O process exhibits potential as an excellent adsorbent for high F-containing geothermal water treatment.

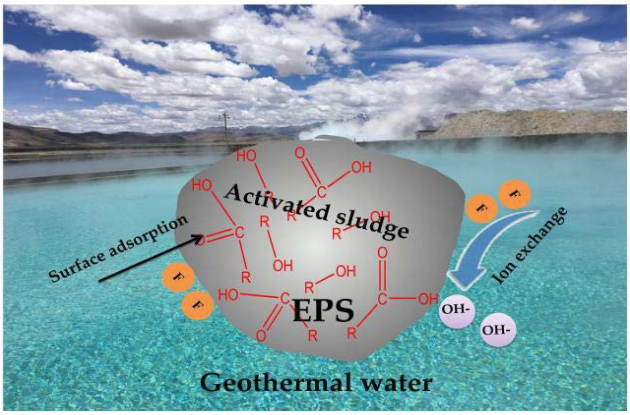

Fig. 8. Proposed mechanism of F^- removal by the activated sludge.

Table 5
Comparison of adsorption capacity (mg/g) on different waste adsorbents

Adsorbents	pH	Equilibrium time	Adsorption capacity (mg/g)	References
Plain carbon	3	5 d	0.49	[33]
Activated peels of selected citrus fruits carbon	7	35 min	0.366–0.391	[34]
Red mud	5.5	2 h	0.164–0.331	[35]
Sludge	6.12	70 min	0.14	[36]
Cashewnut shell carbon	7	180 min	1.83	[37]
Orange waste	3–6	4 h	8.37–22.42	[38]
Activated bael shell carbon	6	60 min	2.4	[39]
Activated cotton nut shell carbon	7	180 min	1.379–3.359	[40]
Apatite materials	5–6	30 min	4.575	[41]
Alum sludge	6	120 min	5.394	[42]
Activated sludge	9.42	180 min	0.55	This work

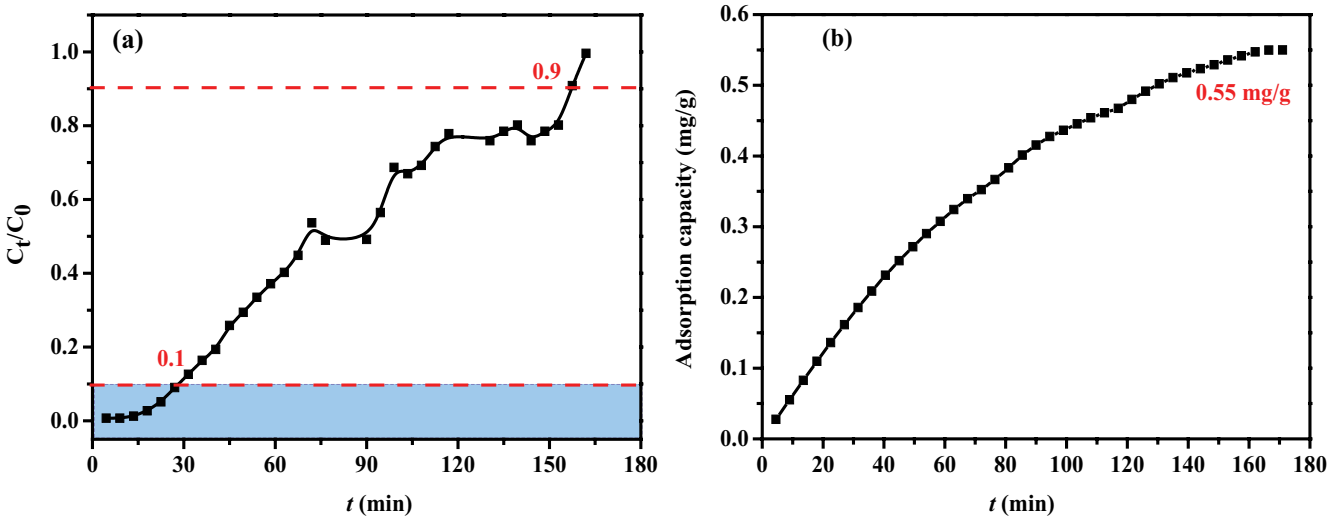

Fig. 9. Variation of C_t/C_0 (a) and adsorption capacity (b).

Acknowledgments

This research was funded by the National Natural Science Foundation of China (22266032), the Second Comprehensive Scientific Investigation Project of Qinghai-Tibet Plateau (2019QZKK0603), High Level Training Programs for Postgraduates of Tibet University (2017-GSP-018), Key Projects of "Science and Technology Help Economy 2020" (SQ2020YFF0423891), State Key Laboratory of Environmental Chemistry and Ecotoxicology, Research Center for Eco-Environmental Sciences, Chinese Academy of Sciences (KF2021-05), 2021 Second Qinghai-Tibet Plateau Scientific Research Support Service and Achievement Transformation Project (XZ202101ZD0014G), Key Projects of Solid Waste Recycling (2019YFC1904103-04), Central Financial Support Special Funds for Local Colleges and Universities ([2021] No. 1, [2020] No.1, [2019] No. 44 and [2018] No.54).

References

[1] Q.H. Guo, Y.W. Cao, J.X. Li, X.B. Zhang, Y.X. Wang, Natural attenuation of geothermal arsenic from Yangbajain power plant discharge in the Zangbo River, Tibet, China, Appl. Geochem., 62 (2015) 164–170.
[2] Q.H. Guo, Y.X. Wang, W.B. Liu, As and F contamination of river water due to wastewater discharge of the Yangbajing geothermal power plant, Tibet, China, Environ. Geol., 56 (2008) 197–205.
[3] S. Jagtap, M.K. Yenkie, N. Labhsetwar, S. Rayalu, Fluoride in drinking water and defluoridation of water, Chem. Rev., 112 (2012) 2454–246.
[4] J. Singh, P. Singh, A. Singh, Fluoride ions vs removal technologies: a study, Arabian J. Chem., 9 (2016) 815–824.
[5] Q.H. Guo, Hydrogeochemistry of high-temperature geothermal systems in China: a review, Appl. Geochem., 27 (2012) 1887–1898.
[6] W.Z. Gai, Z.Y. Deng, A comprehensive review of adsorbents for fluoride removal from water: performance, water quality assessment and mechanism, Environ. Sci. Water Res. Technol., 7 (2021) 1362–1386.
[7] S.V. Jadhav, E. Bringas, G.D. Yadav, V.K. Rathod, I. Ortiz, K.V. Marathe, Arsenic and fluoride contaminated groundwaters: a review of current technologies for contaminants removal, J. Environ. Manage., 162 (2015) 306–325.
[8] Meenakshi, R.C. Maheshwari, Fluoride in drinking water and its removal, J. Hazard. Mater., 137 (2006) 456–463.
[9] X.Y. Hu, F. Zhu, L.H. Kong, X.J. Peng, A novel precipitant for the selective removal of fluoride ion from strongly acidic wastewater: synthesis, efficiency, and mechanism, J. Hazard. Mater., 403 (2021) 124039–124045.
[10] J.J. Garcia-Sanchez, M. Solache-Rios, V. Martinez-Miranda, Removal of fluoride ions by calcium hydroxide-modified iron oxides, Desal. Water Treat., 94 (2017) 31–39.
[11] Z.Z. Wu, J.F. Su, A. Ali, X.F. Hu, Z. Wang, Study on the simultaneous removal of fluoride, heavy metals and nitrate by calcium precipitating strain *Acinetobacter* sp. H12, J. Hazard. Mater., 405 (2021) 124255–124260.
[12] D. Tang, G. Zhang, Efficient removal of fluoride by hierarchical Ce–Fe bimetal oxides adsorbent: thermodynamics, kinetics and mechanism, Chem. Eng. J., 283 (2016) 721–729.
[13] J. Wang, D.J. Kang, X.L. Yu, M.F. Ge, Y.T. Chen, Synthesis and characterization of Mg–Fe–La trimetal composite as an adsorbent for fluoride removal, Chem. Eng. J., 264 (2015) 506–513.
[14] J.J. Garcia-Sanchez, M. Solache-Ríos, M.T. Alarcon-Herrera, V. Martinez-Miranda. Removal of fluoride from well water by modified iron oxides in a column system, Desal. Water Treat., 57 (2016) 2125–2133.
[15] J.B. Chen, R.J. Yang, Z.Y. Zhang, D.Y. Wu, Removal of fluoride from water using aluminum hydroxide-loaded zeolite synthesized from coal fly ash, J. Hazard. Mater., 421 (2022) 126817, doi: 10.1016/j.jhazmat.2021.126817.
[16] G. Vazquez-Mejia, M. Solache-Rios, V. Martinez-Miranda, Removal of fluoride and arsenate ions from aqueous solutions and natural water by modified natural materials, Desal. Water Treat., 85 (2017) 271–281.
[17] S.P. Shukla, S. Tiwari, M. Tiwari, D. Mohan, G. Pandey, Removal of fluoride from aqueous solution using *Psidium guajava* leaves, Desal. Water Treat., 62 (2017) 418–425.
[18] O. Gulnaz, A. Kaya, S. Dincer, The reuse of dried activated sludge for adsorption of reactive dye, J. Hazard. Mater., 134 (2006) 190–196.
[19] T. Urase, T. Kikuta, Separate estimation of adsorption and degradation of pharmaceutical substances and estrogens in the activated sludge process, Water Res., 39 (2005) 1289–1300.
[20] Y. Zhou, S. Xia, J. Zhang, Z. Zhang, S.W. Hermanowicz, Adsorption characterizations of biosorbent extracted from waste activated sludge for Pb(II) and Zn(II), Desal. Water Treat., 57 (2016) 9343–9353.
[21] B. Veenhuyzen, S. Tichapondwa, C. Hörstmann, E. Chirwa, H.G. Brink, High capacity Pb(II) adsorption characteristics onto raw- and chemically activated waste activated sludge, J. Hazard. Mater., 416 (2021) 125943–125949.

[22] J. Zeng, J.M. Gao, Y.P. Chen, P. Yan, Y. Dong, Y. Shen, J.S. Guo, N. Zeng, P. Zhang, Composition and aggregation of extracellular polymeric substances (EPS) in hyperhaline and municipal wastewater treatment plants, Sci. Rep., 6 (2016) 26721–26729.
[23] M. Kowalski, K. Kowalska, J. Wiszniowski, J. Turek-Szytow, Qualitative analysis of activated sludge using FT-IR technique, Chem. Pap., 72 (2018) 2699–2706.
[24] M.J. Zhang, J. Yang, H.X. Wang, Q. Lv, J.B. Xue, Enhanced removal of phosphate from aqueous solution using Mg/Fe modified biochar derived from excess activated sludge: removal mechanism and environmental risk, Environ. Sci. Pollut. Res., 28 (2021) 16282–16297.
[25] Z.D. Zhang, Q. Li, X.L. Luo, H.C. Jiang, Q.F. Zheng, L.P. Zhao, J.H. Wang, Research on characteristics of soil clay mineral evolution in paddy field and dry land by XRD spectrum, Spectrosc. Spect. Anal., 34 (2014) 2273–2278.
[26] J. He, T.S. Siah, J.P. Chen, Performance of an optimized Zr-based nanoparticle-embedded PSF blend hollow fiber membrane in treatment of fluoride contaminated water, Water Res., 56 (2014) 88–97.
[27] Z. Jin, Y. Jia, T. Luo, L.T. Kong, J.H. Liu, Efficient removal of fluoride by hierarchical MgO microspheres: performance and mechanism study, Appl. Surf. Sci., 357 (2015)1080–1088.
[28] N.A. Oladoja, S. Hu, J.E. Drewes, B. Helmreich, Insight into the defluoridation efficiency of nano magnesium oxide in groundwater system contaminated with hexavalent chromium and fluoride, Sep. Purif. Technol., 162 (2016) 195–202.
[29] J.C. Burillo, L. Ballinas, G. Burillo, E. Guerrero-Lestarjette, D. Lardizabal-Gutierrez, H. Silva-Hidalgo, Chitosan hydrogel synthesis to remove arsenic and fluoride ions from groundwater, J. Hazard. Mater., 417 (2021) 126070–126076.
[30] M. Wang, X.L. Yu, C.L. Yang, X.Q. Yang, M.Y. Lin, L.T. Guan, M.F. Ge, Removal of fluoride from aqueous solution by Mg-Al-Zr triple-metal composite, Chem. Eng. J., 322 (2017) 246–253.
[31] E. Kumar, A. Bhatnagar, M.K. Ji, W. Jung, S.H. Lee, S.J. Kim, G. Lee, H. Song, J.Y. Choi, J.S. Yang, B.H. Jeona, Defluoridation from aqueous solutions by granular ferric hydroxide (GFH), Water Res., 43 (2009) 490–498.
[32] Y. Liu, Y. Li, X.P. Yan, Preparation, characterization, and application of L-cysteine functionalized multiwalled carbon nanotubes as a selective sorbent for separation and preconcentration of heavy metals, Adv. Funct. Mater., 18 (2008) 1536–1543.
[33] R.L. Ramos, J. Ovalle-Turrubiartes, M.A. Sanchez-Castillo, Adsorption of fluoride from aqueous solution on aluminum-impregnated carbon, Carbon, 37 (1999) 609–617.
[34] C. Chakrapani, B.C. Suresh, K. Vani, K.S. Rao, Adsorption kinetics for the removal of fluoride from aqueous solution by activated carbon adsorbents derived from the peels of selected citrus fruits, J. Chem., 7 (2010) 419–427.
[35] Y. Çengeloğlu, E. Kır, M. Ersöz, Removal of fluoride from aqueous solution by using red mud, Sep. Purif. Technol., 28 (2002) 81–86.
[36] Y. Li, S.K. Yang, Q.L. Jiang, J. Fang, The adsorptive removal of fluoride from aqueous solution by modified sludge: optimization using response surface methodology, Int. J. Environ. Res. Public Health, 15 (2018) 826, doi: 10.3390/ijerph15040826.
[37] G. Alagumuthu, M. Rajan, Equilibrium and kinetics of adsorption of fluoride onto zirconium impregnated cashew nut shell carbon, Chem. Eng. J., 158 (2010) 451–457.
[38] H. Paudyal, B. Pangeni, K. Inoue, H. Kawakita, K. Ohto, H. Harada, S. Alam, Adsorptive removal of fluoride from aqueous solution using orange waste loaded with multi-valent metal ions, J. Hazard. Mater., 192 (2011) 676–682.
[39] K. Singh, D.H. Lataye, K.L. Wasewar, Removal of fluoride from aqueous solution by using bael (*Aegle marmelos*) shell activated carbon: kinetic, equilibrium and thermodynamic study, J. Fluorine Chem., 194 (2017) 23–32.
[40] R. Mariappan, R. Vairamuthu, A. Ganapathy, Use of chemically activated cotton nut shell carbon for the removal of fluoride contaminated drinking water: kinetics evaluation, Chin. J. Chem. Eng., 23 (2015) 710–721.
[41] S. Gao, J. Cui, Z.G. Wei, Study on the fluoride adsorption of various apatite materials in aqueous solution, J. Fluorine Chem., 130 (2009) 1035–1041.
[42] M.G. Sujana, R.S. Thakur, S.B. Rao, Removal of fluoride from aqueous solution by using alum sludge, J. Colloid Interface Sci., 206 (1998) 94–101.